

A Case study of Performance Improvement of Femur Prosthesis

Leila Shahryari ^{a,*}, Behtash JavidSharifi ^b, Mehdi Dabaghmanesh ^c

^aAssociate Professor, Islamic Azad University, Shiraz Branch (Corresponding Author)

^bConstruction Superintendent, Design & Development Department, Fars Regional Electric Company (FREC)

^cM.Sc. of Structural Engineering, Islamic Azad University, Shiraz Branch

Received 17 March 2019, Accepted 09 June 2020

Abstract

Nowadays, the placement of artificial prostheses in human skeleton, etc. is common due to different reasons such as fractures or deficiencies. Prostheses are structures that assist the performance of organs by reconstruction of some body parts through different methods to enable the organ to re-obtain its performance completely or partially and, since the use of external prostheses might lead to issues such as severe traumas, slow recovery, and imposition of enormous hospital costs on the patient, therefore, use of internal prostheses can be an effective method for accelerating the process of improvement for the patient. By using CT-scan photos of a 54-year-old man weighing 60 kg and with a femur length of 36 centimeters, and also using a titanium prosthesis with diameters equaling 9 and 13 mm along with screws with diameters of 4 mm whose placement are with angles of ± 4 , ± 4 and ± 36 degrees, the geometry of the model has been provided and the model has been analyzed through the finite element method. Results indicated that in case of using the prosthesis with a diameter of 13 mm and screws of 4 mm with an angle of $+36$, the least stress will be imposed on the bone and prosthesis.

Keywords: Artificial prosthesis, Femur, Geometric modeling, Finite element analysis.

1. Introduction

The placement of a part of bone via an implant can decrease the pains caused by different joint-bone diseases. Nowadays, this is widely done through about 800,000 surgeries yearly and is the second most common operation after dental surgeries worldwide. The success or failure of this type of surgery is severely dependent upon the design of the implants. Therefore, acceptance of a new design and its extensive production, and the issuance of permission for its use in a surgery depend on laboratory tests and even computer modeling and analysis for confidence and satisfactory design results [1].


There are different steps that must be considered for the design of femur prostheses, whose most important ones include [2]:

1. Covering the sizes and bone figures of a wide range of patients with different anatomical features,
2. Mechanical and kinematical stability under

physiological loads that have cyclic nature,

3. Proof of ability to provide the required range of motion.

In the top part of the Acetabulum area, the femur is joined to the hip bone and its other end is joined to the knee area through the patella bones. The femurs are the two longest bones in the human body while they are also the strongest and largest ones. The length of the human femur is generally about 36 cm, give or take, and its diameter is 2.34 cm. On average, this bone can typically bear up to 36 times more than the weight of an adult. The top part of the femur (also called the femur head) is round and sphere-shaped and it is joined to the lower shaft via a connecting bone section called the 'neck of femur.' The angle between the neck and body of the femur is significant and some diseases get changed. This angle is naturally about 125 degrees. The fracture of the femur neck, which is usually seen in elder people caused proceeding osteoporosis, usually needs surgery [3].

 *Corresponding Author: Email address: lshahryari@alumni.iust.ac.ir

Lower than the head of the femur there are two other flanges, namely the Greater Trochanter and the Small Trochanter. These two flanges are the junction of strong hip muscles. At the end of the distal bone are the internal and external condyles that are located in the knee area (see Figures 1 to 4) [4].



Fig.1. Schematic view of the femur [20]



Fig. 2. Front view X-ray of the lower part of the femur



Fig. 3. Front view X-ray of the upper part of the femur



Fig. 4. Side view X-ray of the upper part of the femur

A controlling step in the design of a bone prosthesis is to choose the appropriate material. This material must be well adaptive with the host tissues, neighboring parts and even, on a farther scale, with all parts of the body. Some implants must remain in the body for good. The geometric shape of prostheses are significant due to the way of their transferring of the loads and their patterns of stress distribution from and to the nearby bones and the mutual surface of different phases of the implant-bone systems. This issue in joint prostheses provides the range of motion and cinematic stability [5]. If an implant with a suitably low-hardness material whose hardness is close to that of the trabecular bone can be designed, the stress distribution pattern in the bone will become more uniform and considerably fewer relative and unfavorable movements between the implant and the adjacent bones could be induced [6]. Therefore, more loads can be proximally transferred to the femur by changing the constituting material of the prosthesis and, e.g., using a titanium alloy instead of chrome-cobalt alloys [7].

An Important step in finite element modeling of the bone is to establish a geometric model that can be identifiable in the selected finite element software program. Then, regarding the features of each area of the model and the required accuracy of the problem, the appropriate element type is chosen and the model meshes. Next, by considering the natural features of the problem media, the boundaries and their appropriate conditions are applied to the model [12, 13, 14 & 22]. Regarding the fact that use of internal prostheses has recently become prevalent (a progression whose major motif has been to decrease the costs as well as retrieve the physical trauma as much as possible), there is still not much information easily able to be gathered about how they are and shall be best modeled.

In this study, using the available standard catalogs, the dimensions and geometry of the typical prosthesis as well as the screws have been extracted and studied in two diameters of 9 and 13 mm (Figure 5), and different angles and stress patterns extension have been considered.



Fig. 5.

Synthesis prosthesis [8]

2. Anatomic modeling

Bones are strong structures the ensemble of which, which is named the skeleton, is considered as the most significant biological and biomechanical structure of the body. One of the significant duties of the skeleton system is to bear and suitably transfer the loads on the body to the ground while

preserving balance. Therefore, when a bone is broken, it is necessary to reinforce the injured area until its complete recovery and strength re-obtaining. One of the methods that are nowadays used for maintaining the efficiency of fractured bones is the replacement of the fractured part with a kind of enforcer or artificial fixator (prosthesis), which is a very common procedure for the case of fractured femurs (Figure 6) [9, 16 & 19].

In this study, in order to establish a geometric model for the prosthesis-therapy procedure of the whole femur, the femur bone material and the screws, first, CT scan photos of a femur bone with IGES and SAT formats were provided and imported into the 3D-Max software. Then, by having the scales of the points defining the geometry of the femur bone, the femur model mesh was created in the software. In the next step, the model was exported to the CATIA software with the SAT format for anatomic modeling. In this software program, modeling was performed by creating the prosthesis and the screws followed by determining the placement of the screws in the femur (Figure 7).

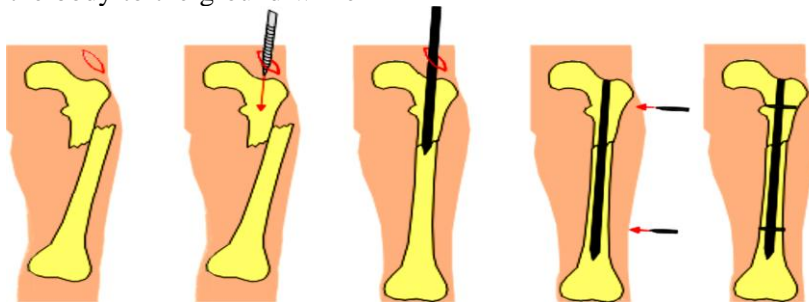


Fig. 6. Schematic view of fractured femur re-assembled with the help of a typical prosthesis [9]

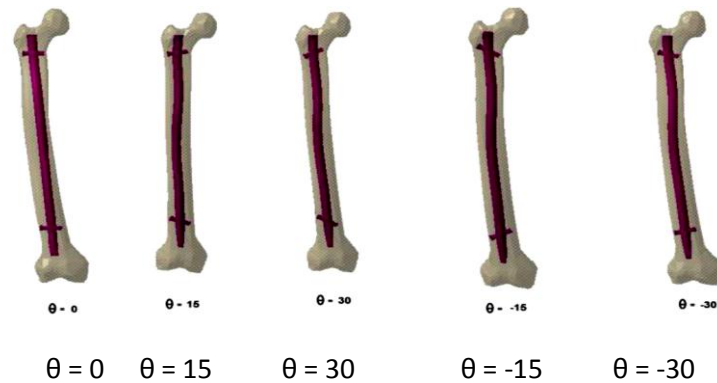


Fig. 7. Femur and prosthesis with different bolt direction angles in CATIA

3. The Finite Element Model and Analysis

Loading, application of the boundary conditions and model analysis were performed in the ABAQUS software program. After developing the geometric models of the prosthesis with different installation angles and femur bones, C3D10 elements were used for meshing. Figure 8 illustrates a schematic view of the 4-node C3D10 element.

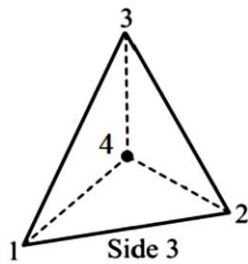


Fig. 8. Triangular 4-node C3D10 element

In order to decrease the computational cost of the finite element analysis of the model, the mechanical features of all model phases were considered as homogeneous and linearly elastic, and the assumed constant Young's modulus of elasticity and Poisson's were taken as presented in Table 1. Therefore, in order to assign the corresponding materials to the whole model, an overall of two materials, namely that of the bone and that of the prosthesis titanium, were defined (Table 1) [24].

After establishing the model and application of the boundary conditions, loading and meshing (as depicted in Figure 9), the analysis of the models was performed. The CT-scan photos were taken from a 54-year-old man leg with an overall weight of 60 kg and a femur length of 36 cm. It is assumed that each thigh bone alone shall have the ability to carry the whole weight of the full body and, hence, the full weight load is given to the single femur (see Figure 9). In addition, the titanium prostheses were taken in accordance with the standard catalogs of the SYNTHES Company [10 & 15] with diameters of 9 and 13 mm and with a net shaft length of 20 cm. Furthermore, the diameter of the assumed screws was 4 mm and

their placement angles were 0.0, ± 5 , ± 15 and ± 30 degrees.

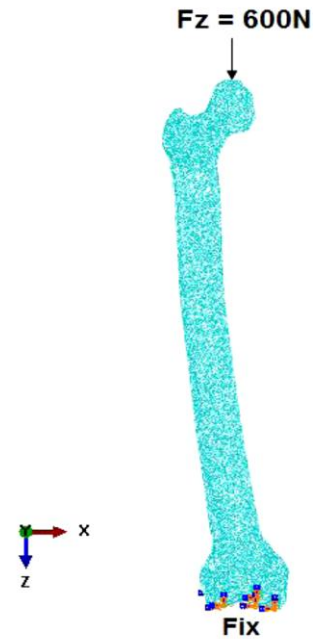


Fig.9. Bone boundary conditions and applied load modeled in ABAQUS

Table 1
Material properties input to the ABAQUS software [21]

Material Type	$E \left(\frac{N}{m^2} \right)$	ν (Poisson's Ratio) (-)
Prosthesis	113.8×10^9	0.342
Bone	17.6×10^9	0.30

4. Evaluation of the Model, Results, and Discussion

Choosing of the prosthesis was done based on the available standards regarding the material, the size of the nail and the size of the screws [10, 11, 17, 18 & 23]. Also, the choice of the screws installation angles (see Figure 10) is such that the changes in the behavior of the prosthesis based on the applied stresses can be clearly seen.

All models were prepared and analyzed separately. The related results of the analyses of the 9- and 13-mm prostheses are given in Tables 2 and 3. Also, Prosthesis and bolt stresses and safety factors for both 9- and 13-mm diameter models are given in Tables 4 and 5.

Ghasemi et al. (2019) reported that, for a 60-year-old person, the mean principal stress of the tibia falls between 14.1 and 82.93 MPa [25], whose range verifies the bone stresses achieved and reported in the tables above.

As is known from structural analysis, in indeterminate structures, the members' internal forces absorbed from the applied external forces are proportionate to the members' stiffnesses which are in turn dependent on the members' moduli of elasticity. A look over the tables and a comparison of the stresses in the prostheses and the vicinity bones reveal that the highest stress has been induced in the prosthesis itself, which can be due to its very high elasticity modulus compared to that of the bone. Such behavior is also justifiable with respect to Hook's law. When the strain in the interface of two objects is constant and, hence, equal for both, in the object with the higher elasticity modulus, stress shall be more too. It is also seen that by increasing the angle of the screws (in the negative and positive directions), the stresses in the nail, screw, and bone are decreased and, as a result, the efficiency of the prosthesis is improved. This can be deduced for both of the prostheses (i.e. with diameters of 9 and 13 mm). The connecting screws, as sensitive parts of the prosthesis, are also studied in Figure 11 which

presents the graph of Von Mises stress for a 5-mm-diameter screw in the previously mentioned angle states.

Table 2
Bone, nail and bolt stresses of the 9-mm model

Inclination Angle (Degrees)	Bone Stress (MP _a)	Nail Stress (MP _a)	Bolt Stress (MP _a)
$\theta = 0^\circ$	19.55	35.87	30.60
$\theta = 15^\circ$	14.59	30.94	25.18
$\theta = 30^\circ$	12.83	29.26	23.47
$\theta = -15^\circ$	16.37	32.94	19.62
$\theta = -30^\circ$	14.59	30.58	22.41

Table 3
Bone, nail and bolt stresses of the 13-mm model

Inclination Angle (Degrees)	Bone Stress (MP _a)	Nail Stress (MP _a)	Bolt Stress (MP _a)
$\theta = 0^\circ$	19.55	28.20	30.44
$\theta = 15^\circ$	14.59	24.11	24.59
$\theta = 30^\circ$	12.73	21.50	21.49
$\theta = -15^\circ$	16.29	26.42	30.52
$\theta = -30^\circ$	14.50	23.85	28.33

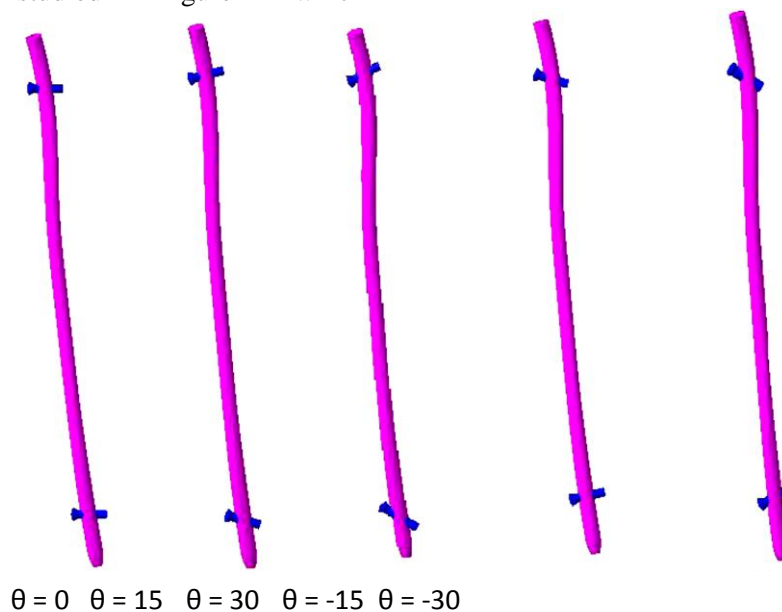


Fig. 10. Bolted prosthesis

Table 4
9- mm prosthesis and bolt stresses and safety factors

Inclination Angle (Degrees)	Nail Stress (MP _a)	Nail Safety Factor ($\sigma_{yield}/\sigma_{Von-Mises}$)	Bolt Stress (MP _a)	Bolt Safety Factor ($\sigma_{yield}/\sigma_{Von-Mises}$)
$\theta = 0^\circ$	35.87	24.25	30.60	28.75
$\theta = 15^\circ$	30.94	28.44	25.18	34.94
$\theta = 30^\circ$	29.26	31.14	23.47	37.94
$\theta = -15^\circ$	32.94	26.71	19.62	29.70
$\theta = -30^\circ$	30.58	28.77	22.41	39.26

Table 5
13-mm prosthesis and bolt stresses and safety factors

Inclination Angle (Degrees)	Nail Stress (MP _a)	Nail Safety Factor ($\sigma_{yield}/\sigma_{Von-Mises}$)	Bolt Stress (MP _a)	Bolt Safety Factor ($\sigma_{yield}/\sigma_{Von-Mises}$)
$\theta = 0^\circ$	28.20	31.20	30.44	28.90
$\theta = 15^\circ$	24.11	38.49	24.59	35.78
$\theta = 30^\circ$	21.50	40.93	21.49	40.94
$\theta = -15^\circ$	26.42	33.30	30.52	28.83
$\theta = -30^\circ$	23.85	36.89	28.33	31.06

With reference to the graph, it can be said that the screw stress in the zero-degree angle is rather at the maximum level. By increasing the angle (in either the positive or negative direction), the maximum stress is decreased. The positive angle is more effective in the reduction of stress. Therefore, the installation of the screws slant in the

positive direction reduces the screws' stress more effectively and, as a result, improves the performance of the prosthesis. Figures 12 and 13 illustrate comparative graphs of stress in the nail and screw for both prostheses (i.e. with diameters of 9 mm and 13 mm):

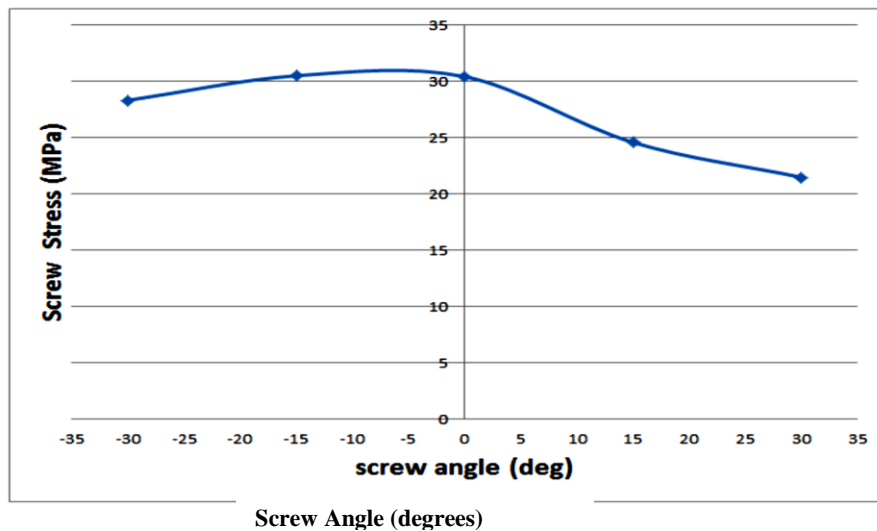


Fig.11. Bolt stresses considering different bolt inclination angles

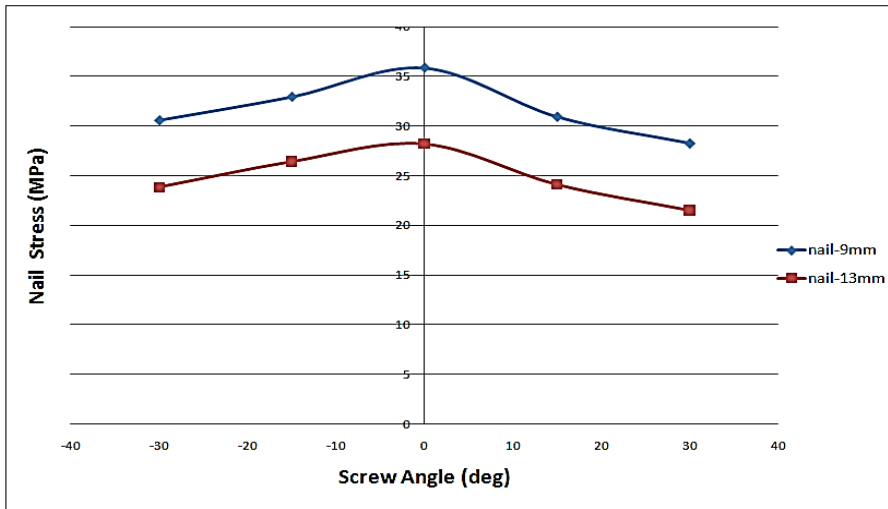


Fig.12: Screw Angle (degrees) diameter prostheses

A comparison of Figure 12 graphs makes it clear that the increase of nail diameter leads to a decrease in the stresses in the prosthesis, which results in an increase in the efficiency of the prosthesis. Also, Figure 12 graphs show that slantwise choosing the angles of screws installation leads to a decrease of the applied stresses on the nail, which is the reason that, by installing the screws with an inclined position, the force is distributed over and carried by a wider contact surface. Also, implementing the screws

with positive installation angles decreases the stresses applied on the nail more effectively, but the equal diameters of the screws in both modes let no tangible change in the screws' stresses take place. Figures 14 to 22 illustrate the stress contours the bone, nail and bolts of bolt models based on the ABAQUS model analysis results.

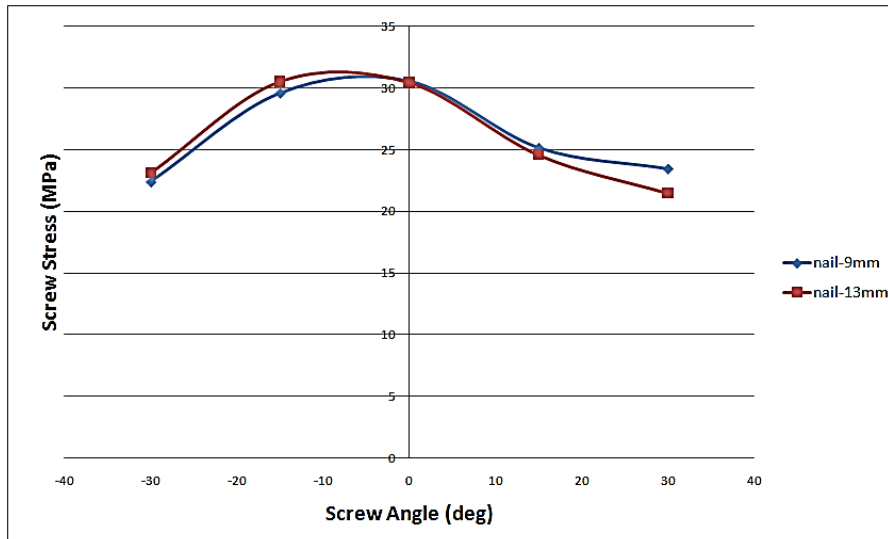
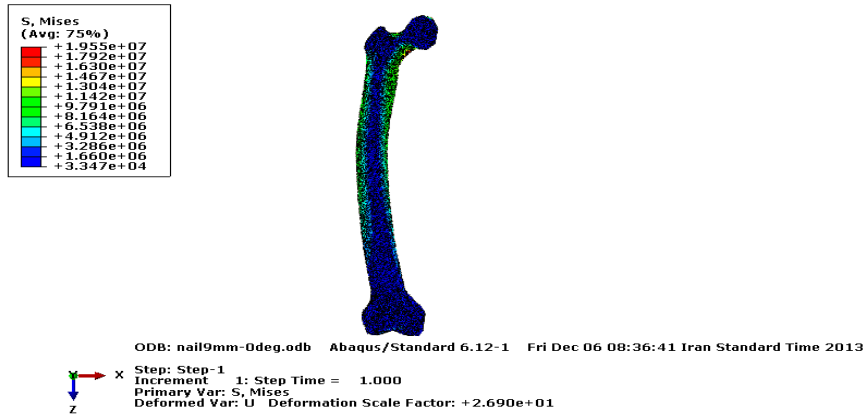
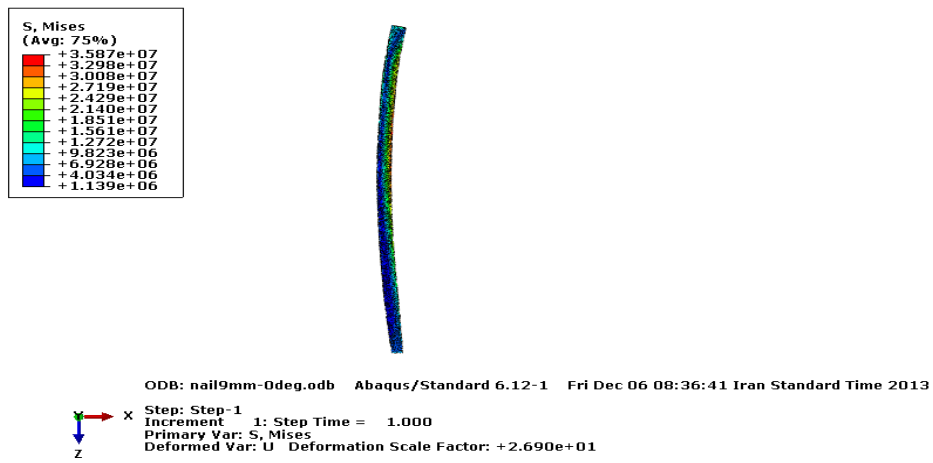


Fig.13. Bolt stresses in 9- and 13-mm diameter prostheses

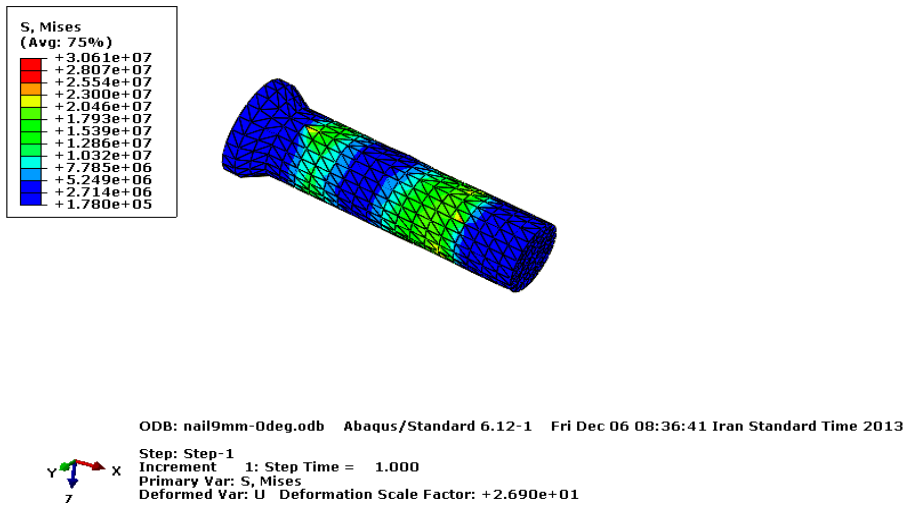
Screw Angle (degrees)



(a)

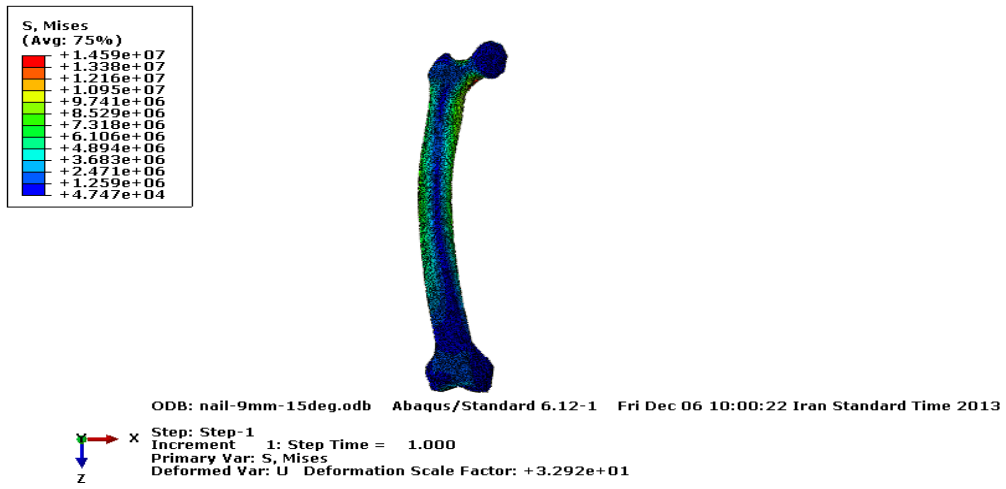


(b)

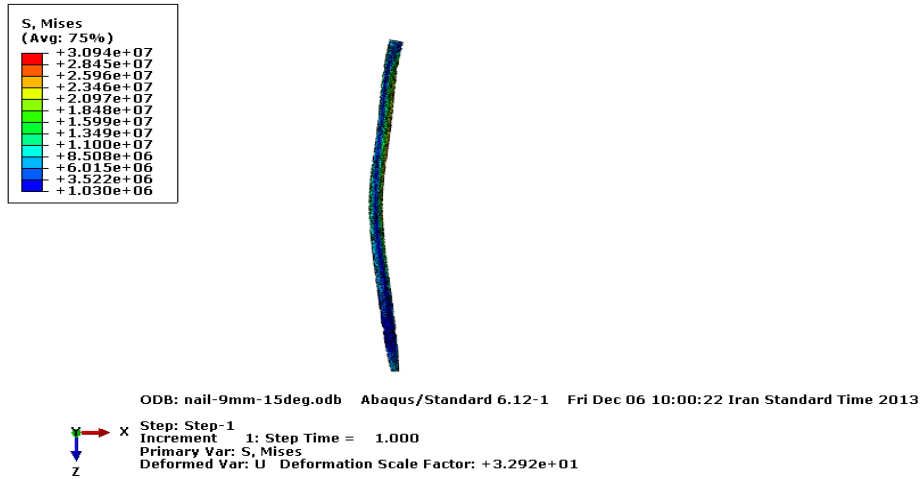


(c)

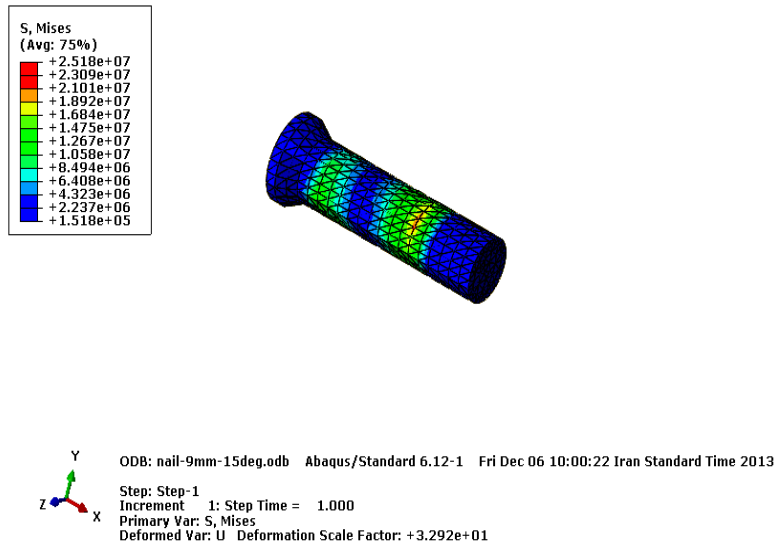
Fig. 14. 9-mm prosthesis model stress contours when $\theta = 0^\circ$, (a) Femur, (b) Nail, (c) Bolt



(a)

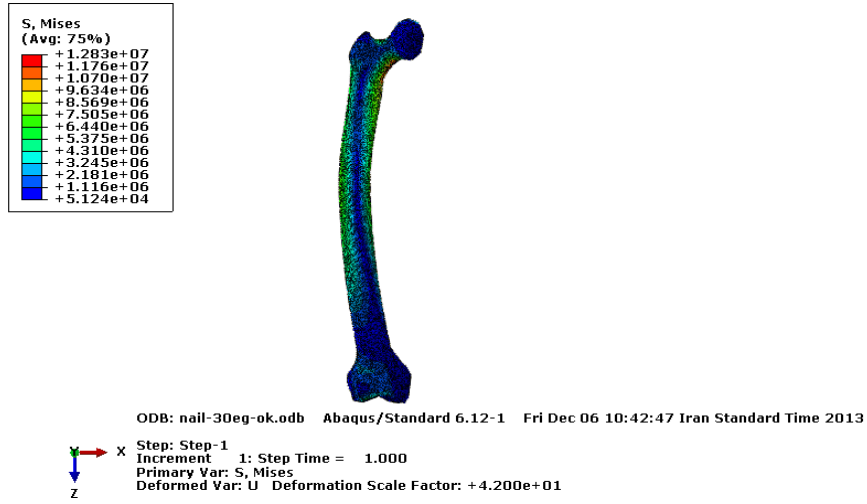


(b)

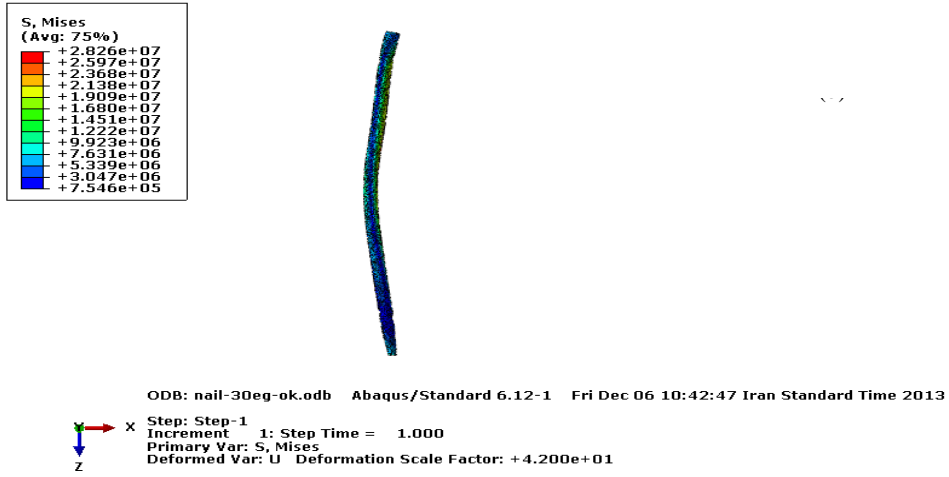


(c)

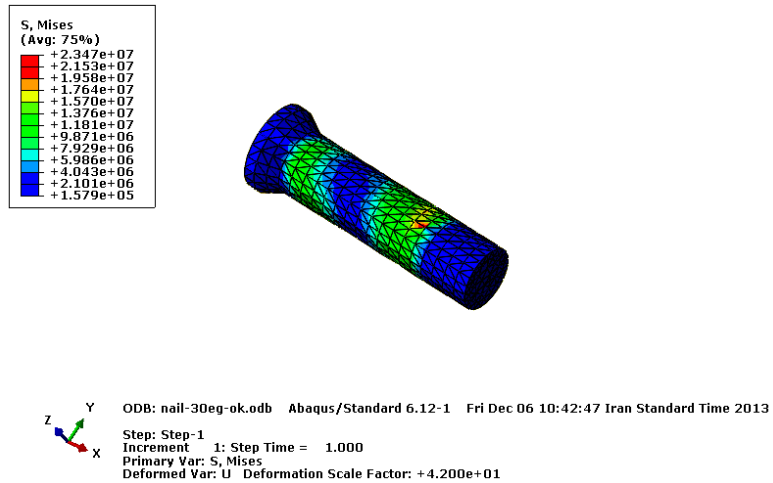
Fig. 15. 9-mm prosthesis model stress contours when $\theta = 15^\circ$, (a) Femur, (b) Nail, (c) Bolt



(a)

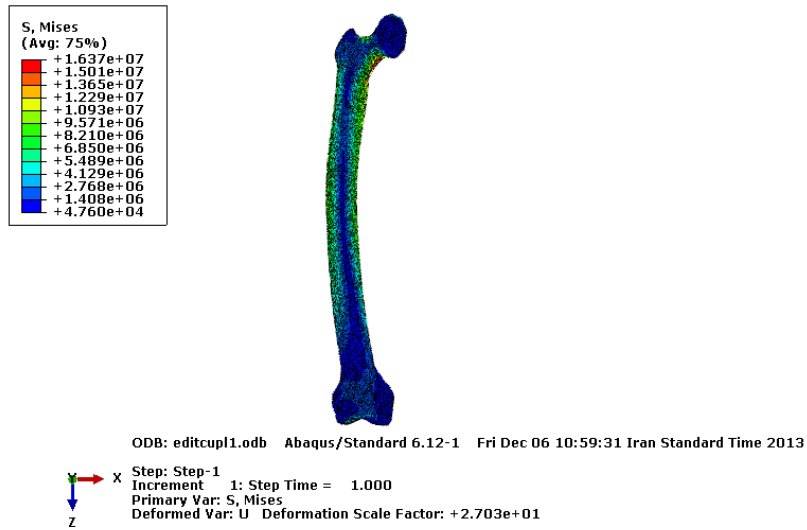


(b)

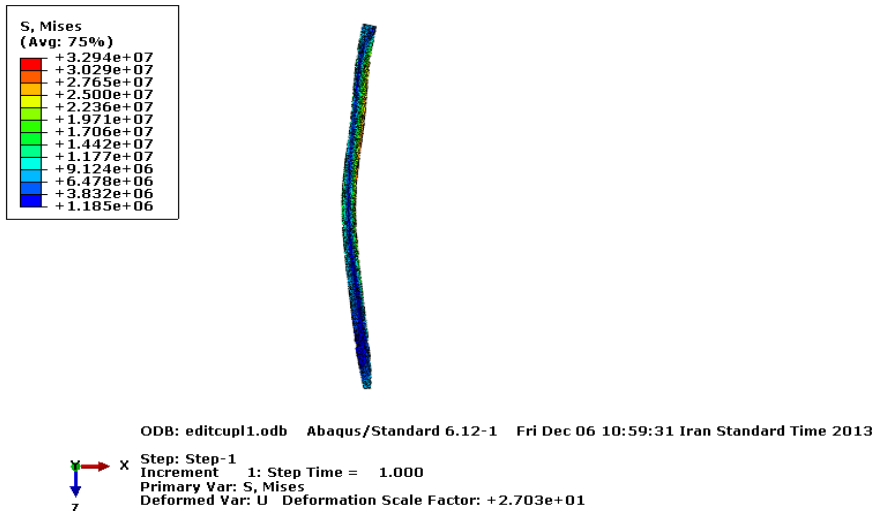


(c)

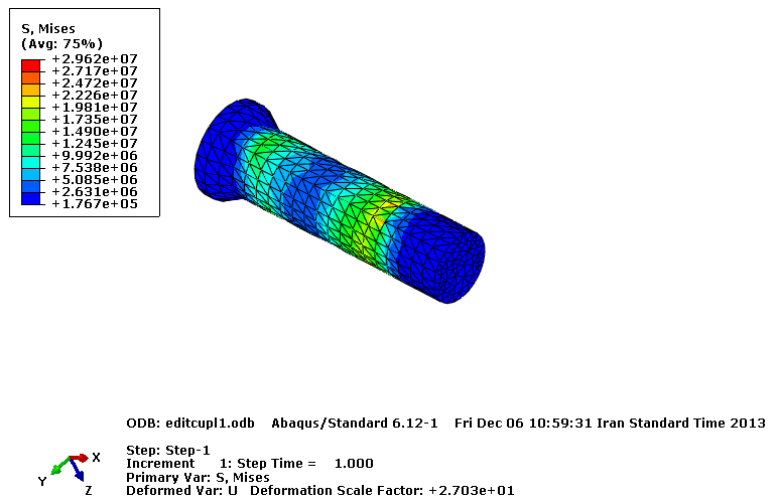
Fig 16. 9-mm prosthesis model stress contours when $\theta = 30^\circ$, (a) Femur, (b) Nail, (c) Bolt



(a)

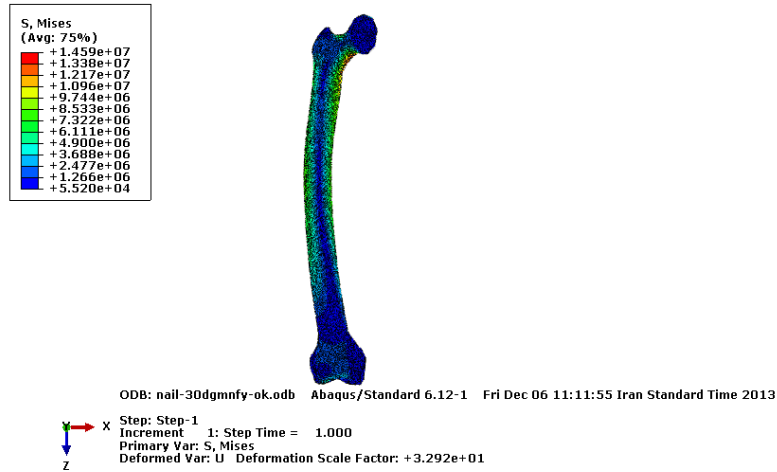


(b)

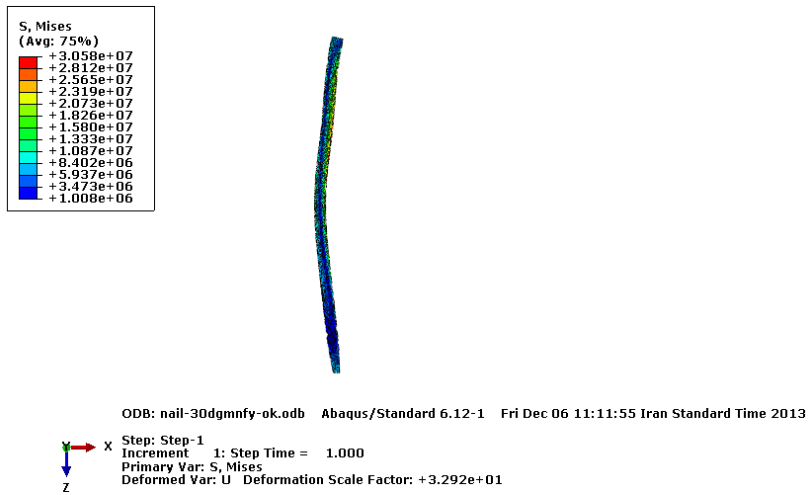


(c)

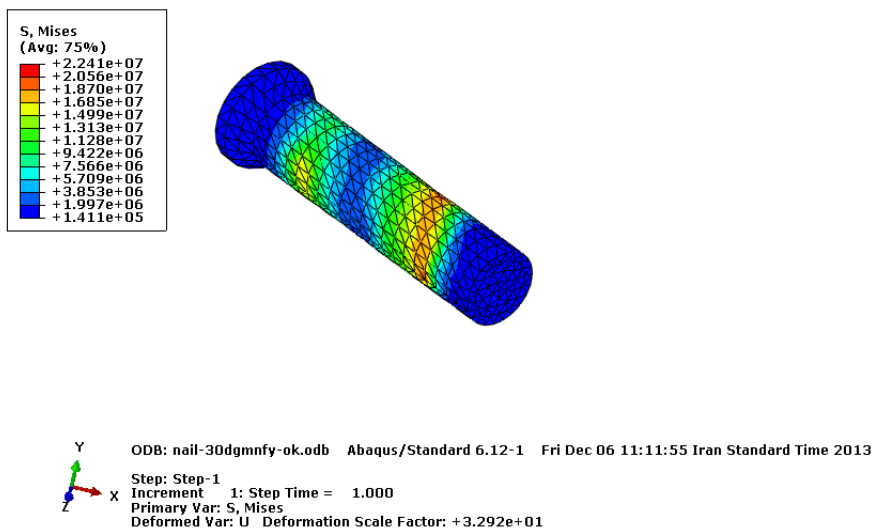
Fig.17. 9-mm prosthesis model stress contours when $\theta = -15^\circ$, (a) Femur, (b) Nail, (c) Bolt



(a)

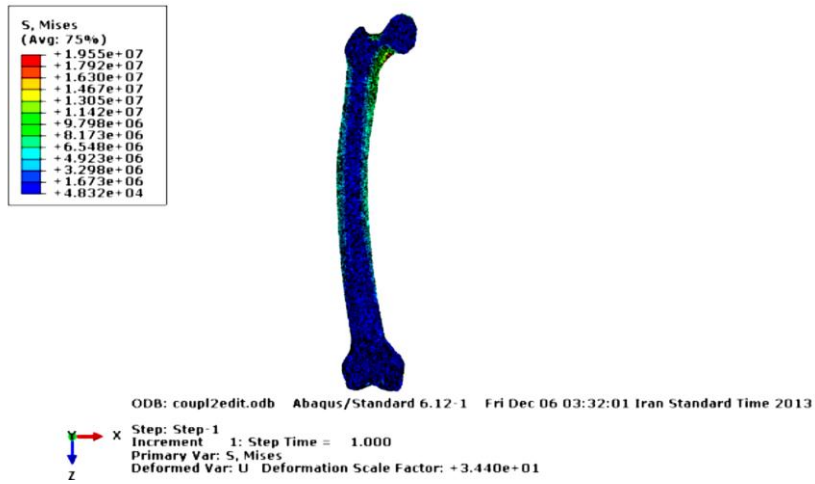


(b)

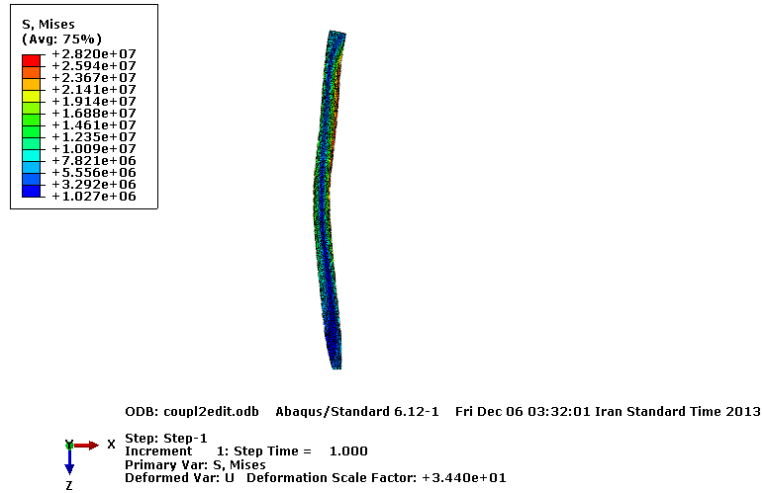


(c)

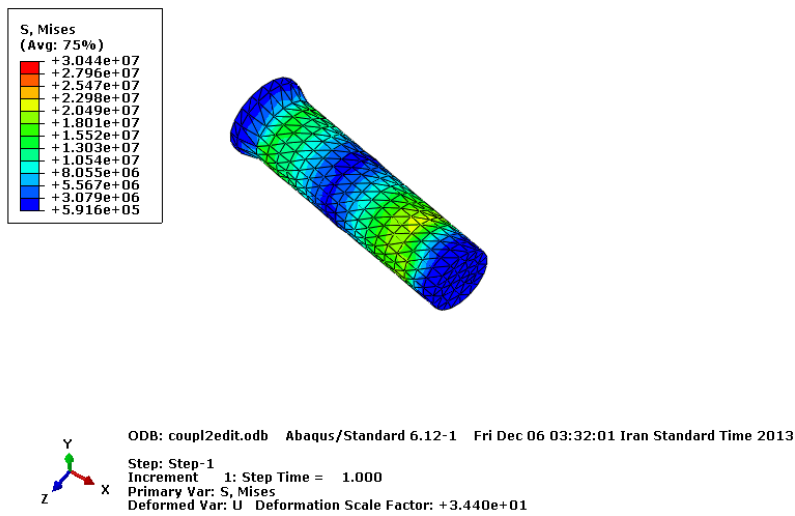
Figure 17. 9-mm prosthesis model stress contours when $\theta = -30^\circ$, (a) Femur, (b) Nail, (c) Bolt



(a)

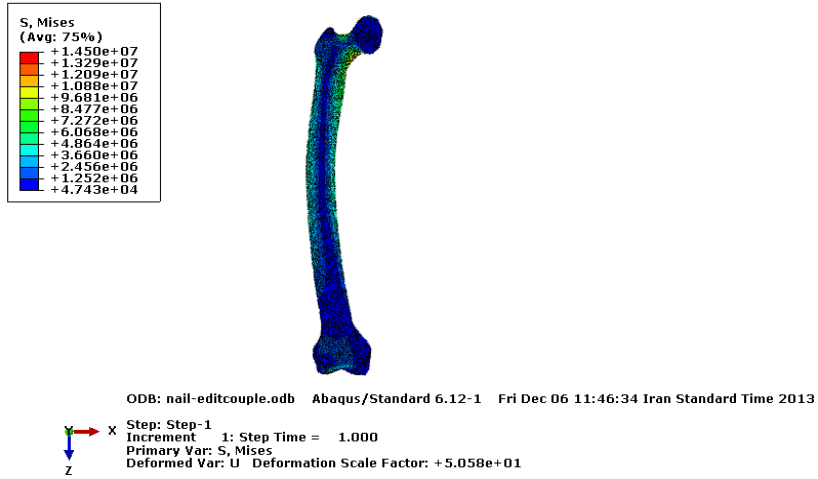


(b)

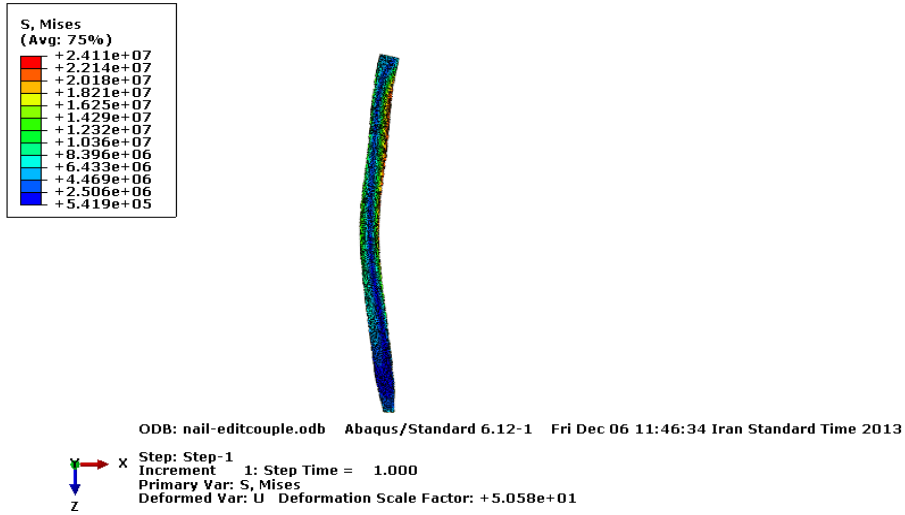


(c)

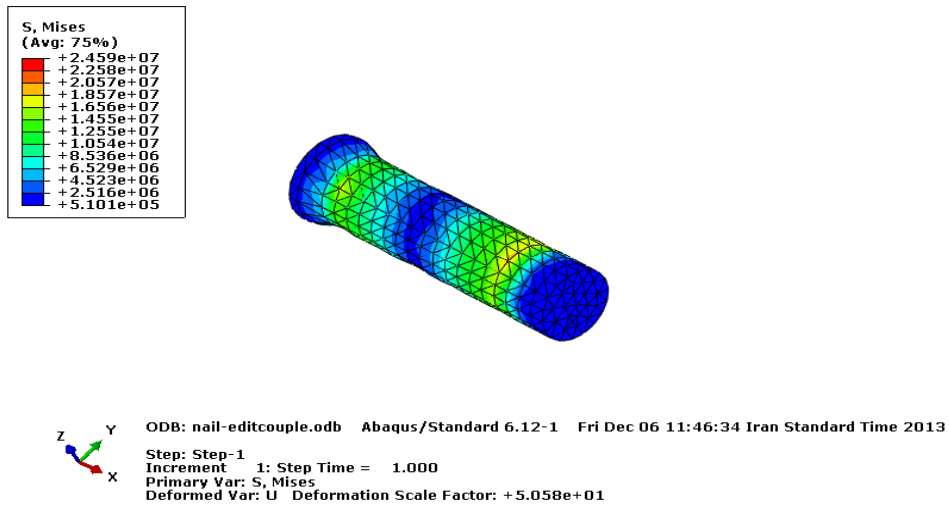
Fig.18.13-mm prosthesis model stress contours when $\theta = 0^\circ$, (a) Femur, (b) Nail, (c) Bolt



(a)

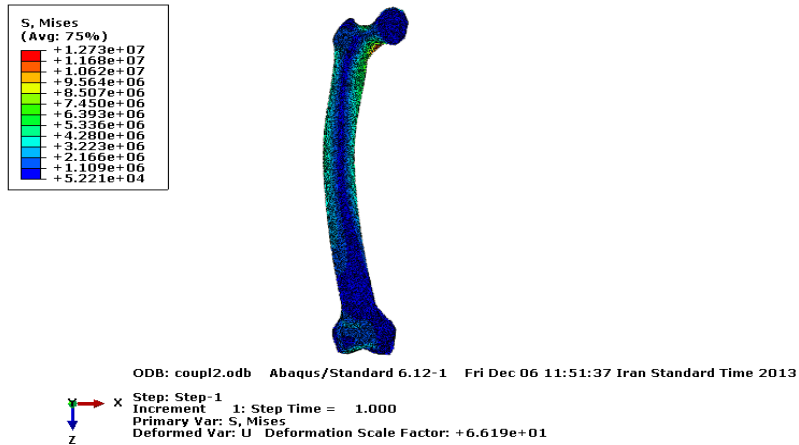


(b)

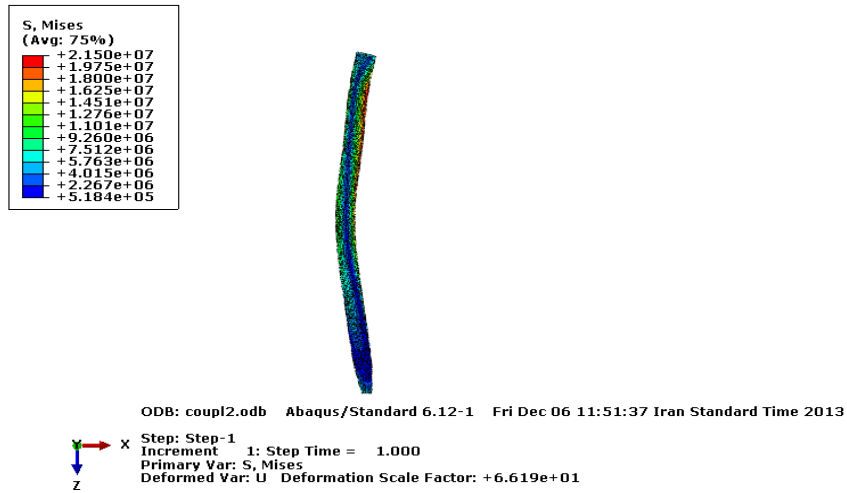


(c)

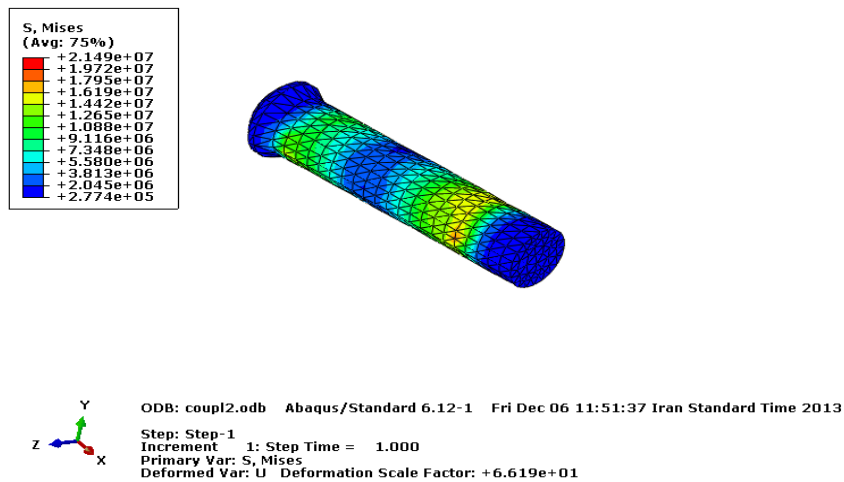
Fig.19.13-mm prosthesis model stress contours when $\theta = 15^\circ$, (a) Femur, (b) Nail, (c) Bolt



(a)

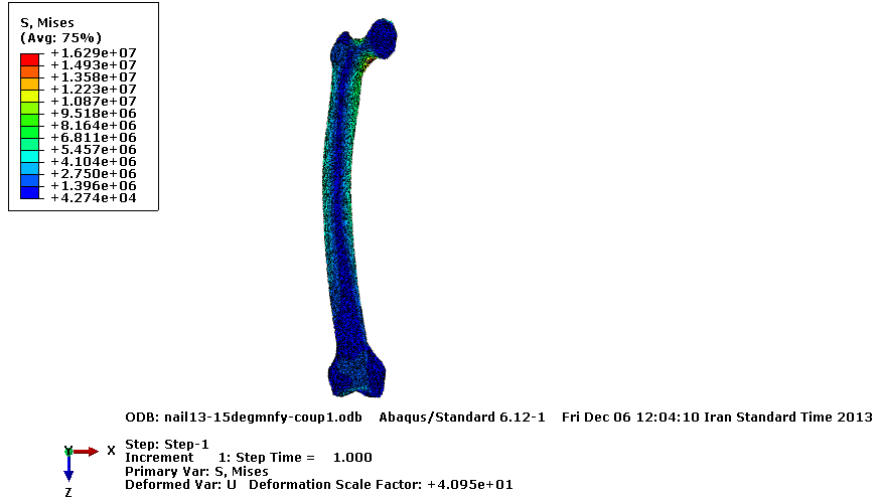


(b)

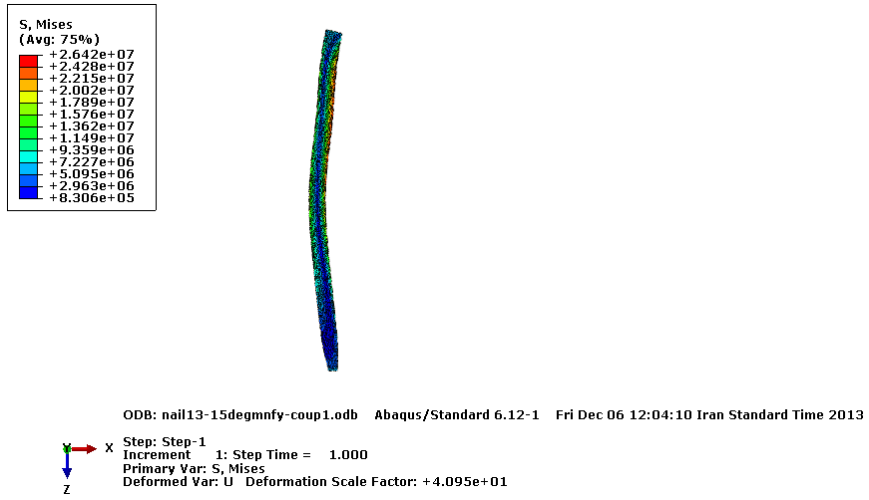


(c)

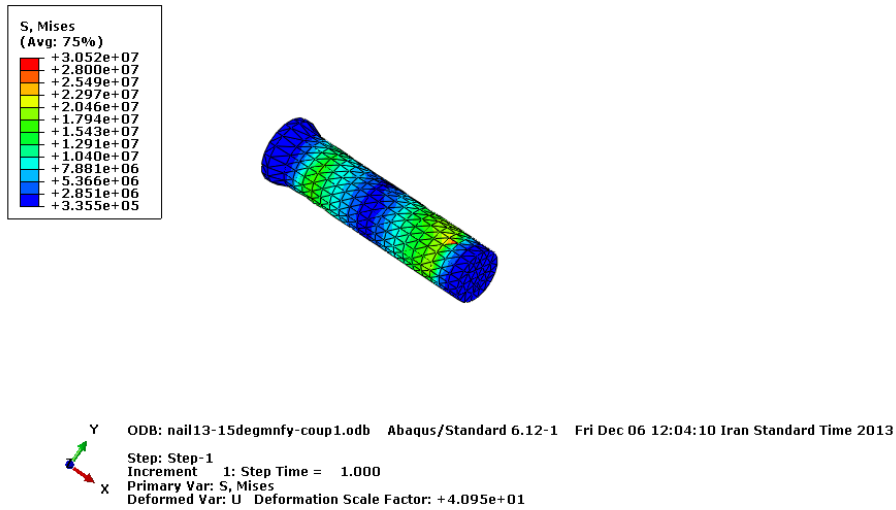
Fig. 20. 13-mm prosthesis model stress contours when $\theta = 30^\circ$, (a) Femur, (b) Nail, (c) Bolt



(a)

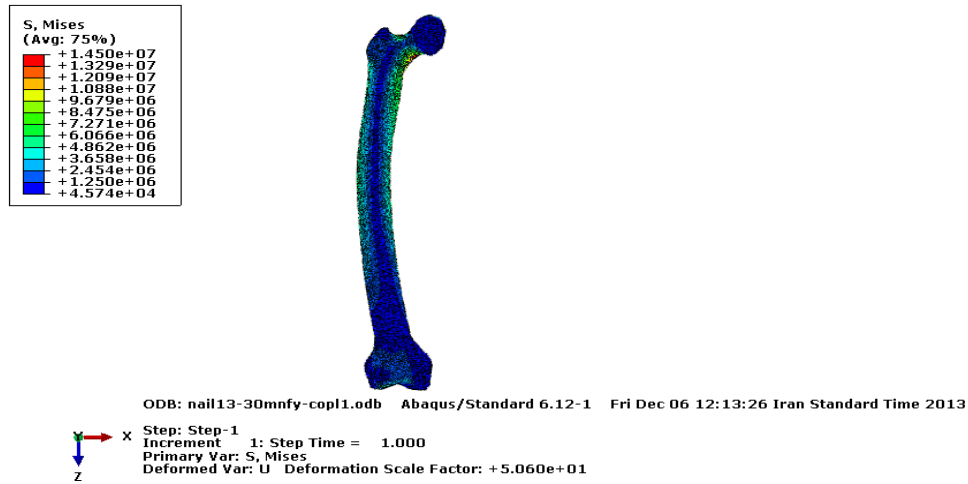


(b)

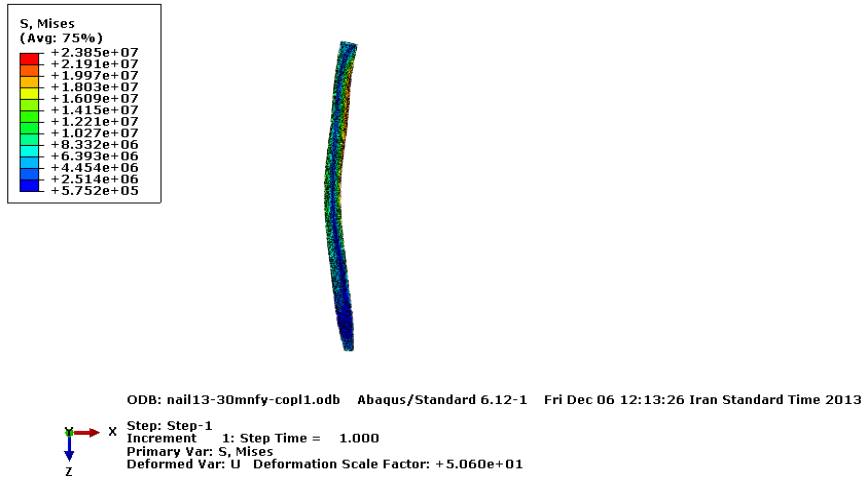


(c)

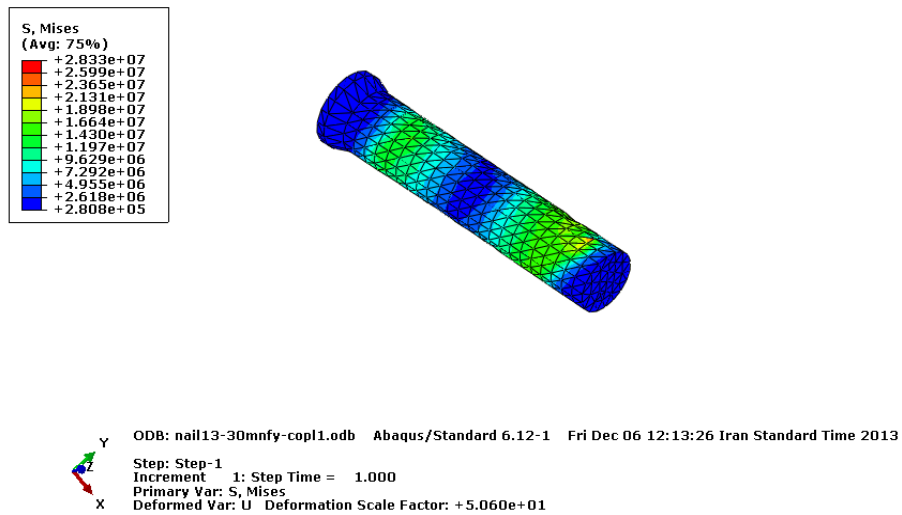
Fig. 21. 13-mm prosthesis model stress contours when $\theta = -15^\circ$, (a) Femur, (b) Nail, (c) Bolt



(a)



(b)



(c)

Fig.22. 13-mm prosthesis model stress contours when $\theta = -30^\circ$, (a) Femur, (b) Nail, (c) Bolt

5. Conclusions

Since minimizing the trauma and costs for the typical femur-fractured patient by improving the performance of the femur-prosthesis has been the purpose of this study, the use of internal titanium prostheses with inclined screws in appropriate angles was investigated. Accordingly, it was observed that the use of the slant screws can cause a lower cost, while, at the same time, it can adequately fulfill the strength and retrieve the trauma. The results of this indicated that in case of using titanium prosthesis with a diameter of 13 mm and screws with diameters of 4 mm and installation angles of +36 degrees, minimal stress is applied to the bone. Therefore, due to the decrease of the injuries caused by surgery as well as reduction of the recovery time, use of this type of prosthesis is recommended for people suffering from femur fractures.

Future researches in this field can include the determination of optimum possible locations of the bolts with respect to the common range of femur lengths. Also, different types of fractures (e.g. when the bone has come to more than two pieces in its length or when one section of the bone has smashed, etc.) shall be taken into account.

References

- [1] Zakeri, N., "Optimization of the femoral prosthesis by finite element method and numerical optimization", Mechanical Engineering MSc. Thesis, Sharif University of Technology, 2004.
- [2] Ashknani, H., "Reliability analysis of artificial femoral joint prosthesis", Mechanical Engineering MSc. Thesis, Sharif University of Technology, 2004.
- [3] Rajaei, M., "General Biomechanics", Publications of Iran University of Science and Technology Press, 2002.
- [4] Amstutz, H.C., "Hip arthroplasty", University of California, Los Angeles (UCLA) Publications, Churchill Livingstone, 1992.
- [5] Cameron, H.U., "Bone implant Interface", Mosby-Year Book Inc. U.S.A, 1994.
- [6] Carter, C.D., Hayes, W.C., "The compressive bone as a two-phase porous structure", Journal of Bone and Joint Surgery, Vol. 59, No. 7, pp. 954-962, 1977.
- [7] Cowin, S.C., "Bone Mechanics" handbook, CRC press.
- [8] Cowin, S.C., Salentijn, M. and Moss, M.L., "Candidate for the mechano-sensory system in bone", Journal of Biomechanics, Vol. 113, pp. 191-197, 1991.
- [9] Cowin S.C., Van Buskrik, W.C. and Ashman, R.B., Handbook of Bioengineering, Chapter 2. "Properties of bone", Editors: Skalak, R., Chien, S., McGraw-Hill, U.S.A, 1987.
- [10] Crenshaw, A.H., "Campbell's Operative Orthopedics" U.S.A., 1991.
- [11] Ganong, W.F., Review of Medical Physiology, 15th edition, Prentice Hall International Inc., U.S.A, 1991.
- [12] Gross, S. and Abel, E.W., "Finite element analysis of hollow stemmed hip prostheses as a means of reducing stress shielding of the femur", Journal of Biomechanics, 34, 995-1003, 2001.
- [13] Halder, A. and Mahadervan, S., "Reliability assessment using stochastic finite element analysis", John Wiley and Sons Inc., 2004.
- [14] Huikes R. and Boeklagen R., "Mathematical shape Optimization of Hip prosthesis Design", Journal of Biomechanics, pp. 22, 793-804, 1989.
- [15] Katoozian, H. and Dwight T. Davy, "Effect of loading conditions and objective function on three-dimensional shape optimization of femoral components of hip endoprostheses", Medical Engineering & Physics 22, pp. 243-251, 2000.
- [16] Katz, J.L. and Meunier, A., "The elastic anisotropy of bone", Journal of Biomechanics, Vol. 20, No. 11/12, PP. 1163-1070, 1987.
- [17] Kim, D.G., Miller, M.A. and Mann, K.A., "Creep dominates tensile fatigue damage of the cement-bone interface", Journal of Orthopedic Research, 22(3), pp. 633-640, 2004.
- [18] Nuno, N. and Avanzolini, G., "Residual stress at the stem-cement interface of an idealized cemented hip stem", Journal of Biomechanics, 35, pp. 849-852, 2002.
- [19] Pawlikowski, M., Skalski, K., and Haraburda, M., "Process of hip Prosthesis design including bone remodeling phenomenon", Computers and Structures, Vol. 81, pp. 887-893, 2003.
- [20] Pope, M.H. and Water, J.O., "Mechanical properties of bone as a function of position and orientation", Journal of Biomechanics. Vol. 7, pp. 61-66, 1974.

- [21] Rho, J.Y., Ashman, R.B. and Turner, C.H., "Young's modulus of trabecular and cortical bone material: ultrasonic and microtensile measurements", *Journal of Biomechanics*, vol. 26, No. 2, pp. 111-119, 1993.
- [22] Stolk, J., Verdonchot, N., Murphy, B.P., Prendergast, P. and Huiskes, R., "Finite element simulation of anisotropic damage accumulation and creep in acrylic bone cement", *Engineering Fracture Mechanics*, 22, pp. 243-251, 2000.
- [23] Viceconti, M., "Wright Medical Technology" Laboratorio di Tecnologia Medica – Istituti Ortopedici Rizzoli, ITALY, viceconti@tecno.ior.it.
- [24] Yong S.Y., Gun H.J. and Young Y.K., "Shape optimal design of the stem of a cemented hip prosthesis to minimize stress concentration in the cement layer", *Journal of Biomechanics* Vol. 22, pp. 1279-1284, 1989.
- [25] Ghasemi, S.H., Kalantari, H., Abdulahi, S.S. and Nowak, A.S. (2019), "Fatigue reliability analysis for medial tibial stress syndrome" *Materials Science & Engineering C*, in press (DOI: <https://doi.org/10.1016/j.msec.2019.01.076>).